R1 in the Shaker S4 occupies the gating charge transfer center in the resting state

Meng-chin A. Lin,[1] Jui-Yi Hsieh,[1,2] Allan F. Mock,[1] and Diane M. Papazian[1,2,3,4]

[1]Department of Physiology, [2]Interdepartmental PhD Program in Molecular, Cellular, and Integrative Physiology, [3]Molecular Biology Institute, and [4]Brain Research Institute, David Geffen School of Medicine, University of California at Los Angeles, Los Angeles, CA 90095

During voltage-dependent activation in Shaker channels, four arginine residues in the S4 segment (R1–R4) cross the transmembrane electric field. It has been proposed that R1–R4 movement is facilitated by a "gating charge transfer center" comprising a phenylalanine (F290) in S2 plus two acidic residues, one each in S2 and S3. According to this proposal, R1 occupies the charge transfer center in the resting state, defined as the conformation in which S4 is maximally retracted toward the cytoplasm. However, other evidence suggests that R1 is located extracellular to the charge transfer center, near I287 in S2, in the resting state. To investigate the resting position of R1, we mutated I287 to histidine (I287H), paired it with histidine mutations of key voltage sensor residues, and determined the effect of extracellular Zn^{2+} on channel activity. In I287H+R1H, Zn^{2+} generated a slow component of activation with a maximum amplitude ($A_{slow,max}$) of ∼56%, indicating that only a fraction of voltage sensors can bind Zn^{2+} at a holding potential of −80 mV. $A_{slow,max}$ decreased after applying either depolarizing or hyperpolarizing prepulses from −80 mV. The decline of $A_{slow,max}$ after negative prepulses indicates that R1 moves inward to abolish ion binding, going beyond the point where reorientation of the I287H and R1H side chains would reestablish a binding site. These data support the proposal that R1 occupies the charge transfer center upon hyperpolarization. Consistent with this, pairing I287H with A359H in the S3–S4 loop generated a Zn^{2+}-binding site. At saturating concentrations, $A_{slow,max}$ reached 100%, indicating that Zn^{2+} traps the I287H+A359H voltage sensor in an absorbing conformation. Transferring I287H+A359H into a mutant background that stabilizes the resting state significantly enhanced Zn^{2+} binding at −80 mV. Our results strongly support the conclusion that R1 occupies the gating charge transfer center in the resting conformation.

INTRODUCTION

In the voltage-gated Shaker K^+ channel, the probability of opening increases from ∼10^{-7} to nearly 1 over a range of <100 mV (Islas and Sigworth, 1999). This exquisite sensitivity to voltage is conferred by positively charged amino acid residues located in the S4 transmembrane segment. In response to membrane depolarization, the side chains of four S4 arginine residues (R1–R4) in each of the four channel subunits are transferred some or all of the way across the transmembrane electric field (Fig. 1 A) (Aggarwal and MacKinnon, 1996; Seoh et al., 1996). These conformational changes convert the voltage sensor domain from its resting state, in which S4 adopts its most inward position, to its fully activated state, in the process transferring ∼13 e_0 across the transmembrane electric field (Schoppa et al., 1992; Aggarwal and MacKinnon, 1996; Seoh et al., 1996; Islas and Sigworth, 1999). How the charged residues cross the transmembrane field is not well understood.

Recently, Tao et al. (2010) proposed that three highly conserved residues, corresponding to F290 and E293 (E2) in S2 and D316 (D3) in S3 in Shaker, constitute a "gating charge transfer center" that facilitates the passage of S4 arginine residues across the transmembrane electric field during activation (Fig. 1, A and B). This charge transfer center is occupied by a lysine residue (K5 in S4) in the x-ray structure of a Kv1.2/Kv2.1 paddle chimera, which depicts the voltage sensor domain in a fully activated or inactivated conformation (Fig. 1 B) (Long et al., 2007). Tao et al. (2010) showed that mutating F290 to tryptophan (F290W) preferentially enhances lysine (K5) occupation of the charge transfer center, stabilizing the activated conformation. In contrast, mutating R1 to lysine and K5 to arginine in the presence of F290W (F290W+R1K+K5R) slows ON gating charge movement and significantly shifts its voltage dependence in the depolarized direction, consistent with stabilizing the resting conformation (Tao et al., 2010). From these results, Tao et al. suggested that R1 occupies the charge transfer center in the resting state.

In contrast, a variety of evidence suggests that R1 is extracellular to F290, in the vicinity of E1 or I287 in S2,

in the resting state (Starace and Bezanilla, 2004; Tombola et al., 2005; Campos et al., 2007). R1 mutations generate gating pore currents carried by protons or monovalent cations (Starace and Bezanilla, 2004; Tombola et al., 2005). These currents, which flow through the voltage sensor domain rather than the central ion-selective pore, are activated by membrane hyperpolarization and are thought to occur in the resting conformation. Mutating E1 in S2 alters the amplitude of gating pore currents, suggesting that R1 is close to E1, above F290, at rest (Tombola et al., 2005). In addition, the R1C mutation in Shaker forms disulfide bonds in the closed state with I241C in S1 or I287C in S2 (Campos et al., 2007). I241 and I287 are located extracellular to the charge transfer center in the paddle chimera structure (Long et al., 2007). These results have been incorporated into models for the resting conformation in which R1 is located above F290, in proximity to E1 in S2 (Yarov-Yarovoy et al., 2006; Campos et al., 2007; Pathak et al., 2007; Khalili-Araghi et al., 2010). This corresponds to the approximate position of R4 in the chimera structure (Long et al., 2007). A recent computational study was able to account for a single-channel gating charge of $\sim$12–12.7 e_0 by converting the paddle chimera structure into a resting state in which R1 in S4 forms a salt bridge with E1 in S2 (Khalili-Araghi et al., 2010).

An important caveat is that most of the experimental evidence supporting current models for the resting state was obtained using R1 mutations (Starace and Bezanilla, 2004; Tombola et al., 2005; Campos et al., 2007). Without the positively charged guanidinium group at the R1 position, S4 may not move as far inward in the mutants as it does in the wild-type channel. However, concerns also apply to the results of Tao et al. (2010) because the combined mutations F290W+R1K+K5R may pull S4 into a deeper position than it normally occupies at rest. Alternatively, the enhanced interaction between F290W and R1K could occur with R1K located above F290W rather than below in the charge transfer center. Therefore, the existing data do not resolve the location of R1 in the resting state.

To investigate the resting position of R1, we have taken advantage of a water-filled crevice that allows extracellular divalent cations to access natural and engineered binding sites in the voltage sensor domain (Silverman et al., 2000, 2004; Tang et al., 2000; Lin et al., 2010). Previously, we showed that mutating I287 in S2 and F324 in S3 to aspartate in Shaker recapitulates a naturally occurring Mg^{2+}-binding site found in eag (Lin et al., 2010). In I287D+F324D, Mg^{2+} shifts the voltage dependence of the delay before channel opening and the initial component of gating charge movement in the depolarized direction. These results support the conclusion that Mg^{2+} binds to and stabilizes the resting state (Silverman et al., 2004; Bannister et al., 2005; Lin et al., 2010). Importantly, the binding site positions 287 and 324 are located extracellular to the gating charge transfer center, as shown in the crystal structure of the paddle chimera (Fig. 1 B).

We now report that R1 in S4 is located in proximity to I287 in an intermediate closed conformation and moves further inward to occupy the gating charge transfer center in the resting state. Our results support a mechanism for Shaker activation in which R1 and K5 are located in the charge transfer center in the resting and activated conformations, respectively, and R2, R3, and R4 traverse this region during voltage-dependent gating.
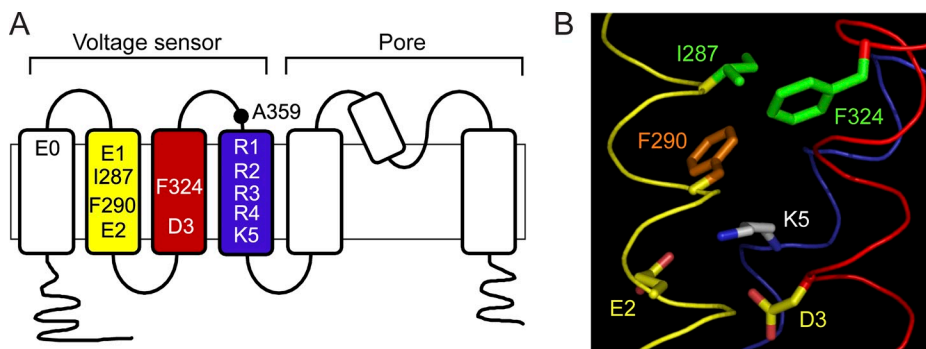

Figure 1. The gating charge transfer center (Tao et al., 2010). (A) The membrane topology of one subunit of the tetrameric Shaker K^+ channel is shown. The approximate positions of conserved charged residues and I287, F290, F324, and A359 in the voltage sensor domain are indicated. Conserved charged residues are labeled using the following generic nomenclature: E0, E247 in S1; E1, E283 in S2; E2, E293 in S2; D3, D316 in S3; R1, R362 in S4; R2, R365 in S4; R3, R368 in S4; R4, R371 in S4; K5, K374 in S4. The S2, S3, and S4 transmembrane segments are shown in yellow, red, and blue, respectively, for comparison to B. (B) The charge transfer center consists of F290 (orange) and E2 in S2 (yellow/red) and D3 in S3 (yellow/red), and is occupied by K5 in S4 (gray/blue) in the Kv1.2/Kv2.1 paddle chimera x-ray structure (Long et al., 2007). Also shown are I287 in S2 and F324 in S3 (green), which correspond to residues that form a naturally occurring binding site for extracellular divalent cations in eag (Silverman et al., 2000; Lin et al., 2010). I287 and F324 are located extracellular to the charge transfer center. Ribbons representing the backbone atoms of S2, S3, and S4 are shown in yellow, red, and blue, respectively. Backbone atoms and the indicated side chains were extracted from the 2r9r x-ray structure and labeled according to the Shaker sequence (Long et al., 2007). In the chimera, the F324 position is occupied by a tyrosine residue, which was mutated in silico using PyMOL (v1.3; The PyMOL Molecular Graphics System; Schrödinger LLC). The figure was made using PyMOL.

MATERIALS AND METHODS

Site-directed mutations were generated in Shaker–inactivation removed (IR; Δ6-46) using QuikChange (Agilent Technologies) and confirmed by sequencing (Hoshi et al., 1990). RNA was transcribed in vitro using the mMessage mMachine T7 Ultra kit (Invitrogen) and injected into oocytes isolated from *Xenopus laevis* frogs. Animal procedures were approved by the Chancellor's Animal Research Committee at UCLA. 1–2 d after injection, ionic currents were recorded at room temperature using a two-electrode voltage clamp (OC-725; Warner Instruments) (Timpe et al., 1988; Papazian et al., 1991). The bath solution contained 96 mM NaCl, 2 mM KCl, 0.5 mM $CaCl_2$, and 5 mM HEPES, pH 7.5, with or without 50 nM to 200 µM $ZnSO_4$, as indicated. Linear leak and capacitive currents were subtracted using a P/−4 protocol.

Activation kinetics were characterized by fitting current traces with one or the sum of two exponential functions using the equations: $y = A[1 - \exp(-t/\tau_{act})] + A_0$ or $y = A_{fast}[1 - \exp(-t/\tau_{fast})] + A_{slow}[1 - \exp(-t/\tau_{slow})] + A_0$, where A corresponds to amplitude and τ corresponds to time constant. A_0 is the initial amplitude, and t is time. To estimate the half-maximal effective concentration of Zn^{2+} ($[Zn^{2+}]_{1/2}$), A or τ values were plotted versus $[Zn^{2+}]$. Datasets were fitted with a rectangular hyperbolic function of the form: $y = P_1 * [Zn^{2+}] / (P_2 + [Zn^{2+}])$, where y corresponds to A or τ, P_1 corresponds to the maximum value of A or τ, and P_2 corresponds to $[Zn^{2+}]_{1/2}$.

To estimate the delay before channel opening, the fitted exponential function was extrapolated to the zero current level; the delay was defined as the difference between this time point and the start of the pulse (Perozo et al., 1994; Lin et al., 2010). To characterize the steady-state properties of activation, conductance was calculated from steady-state current amplitudes at a variety of test voltages and normalized to the maximum value obtained during the experiment. Datasets were fitted with a Boltzmann equation of the form: $g/g_{max} = (A_1 - A_2)/\{1 + \exp[(V - V_{1/2})/slope]\} + A_2$.

Values for kinetic and steady-state parameters are provided as mean ± SEM. Statistical significance was evaluated using a one-way ANOVA followed by Student's *t* test.

RESULTS

I287H and F324H form a Zn^{2+}-binding site extracellular to the charge transfer center

To investigate the resting position of R1 in S4, we mutated I287 to histidine (I287H), paired it with histidine
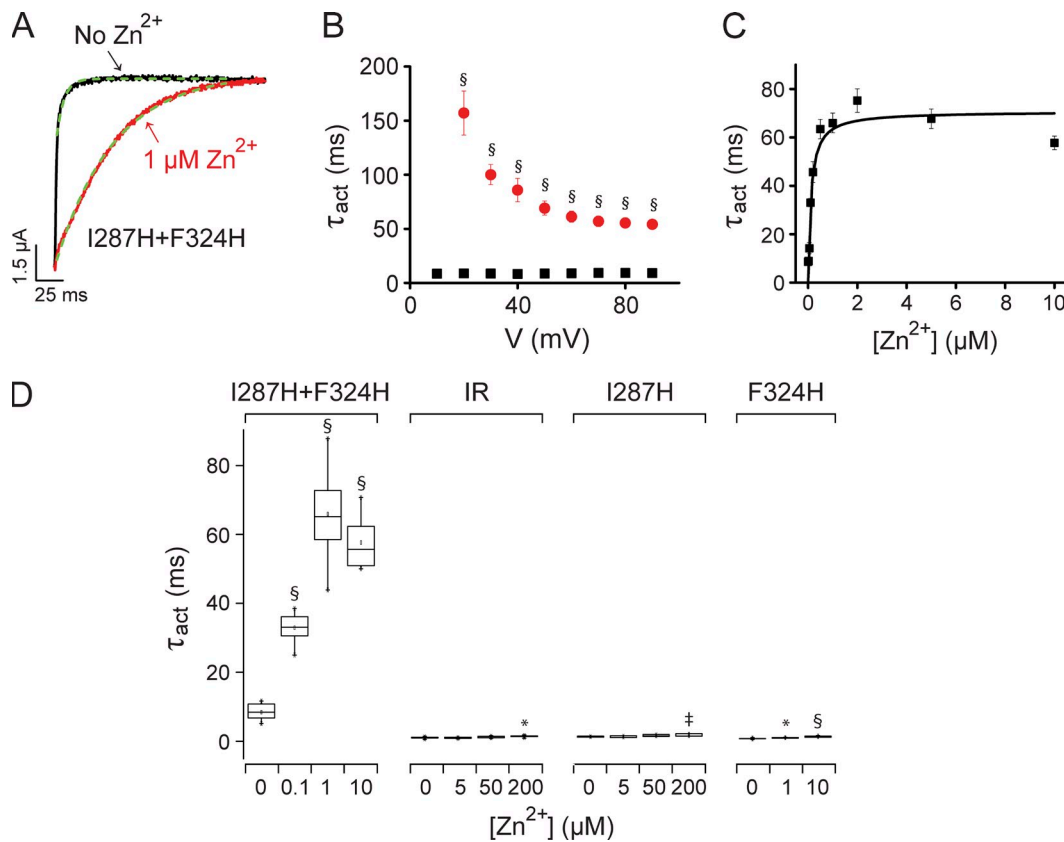

Figure 2. Extracellular Zn^{2+} slows activation in I287H+F324H channels. (A) Currents were evoked by depolarizing from −80 to +60 mV in the absence (black) or presence (red) of 1 µM Zn^{2+}. Traces were fitted with single-exponential functions (dashed green lines) to provide activation time constants (τ_{act}). (B) τ_{act} values measured at test voltages ranging from +10 to +90 mV in the absence (black squares) or presence (red circles) of 1 µM Zn^{2+} differed significantly (§, P < 0.0005) at all voltages. Data are shown as mean ± SEM ($n = 13$). At +60 mV, τ_{act} values were 66 ± 4 ms and 8.6 ± 0.6 ms with and without 1 µM Zn^{2+}, respectively. (C) Values of τ_{act} at +60 mV were plotted versus Zn^{2+} concentration and fitted with a rectangular hyperbola (black line) to determine $[Zn^{2+}]_{1/2}$, which was 0.12 µM ($n = 6–13$). (D) The box plot shows τ_{act} values measured at +60 mV in the indicated concentrations of Zn^{2+} for I287H+F324H, the Shaker-IR parent channel, and the I287H and F324H single-mutant channels. Mean values of τ_{act} that differed significantly from no Zn^{2+} are indicated: *, P < 0.05; ‡, P < 0.005; §, P < 0.0005 ($n = 2–13$).
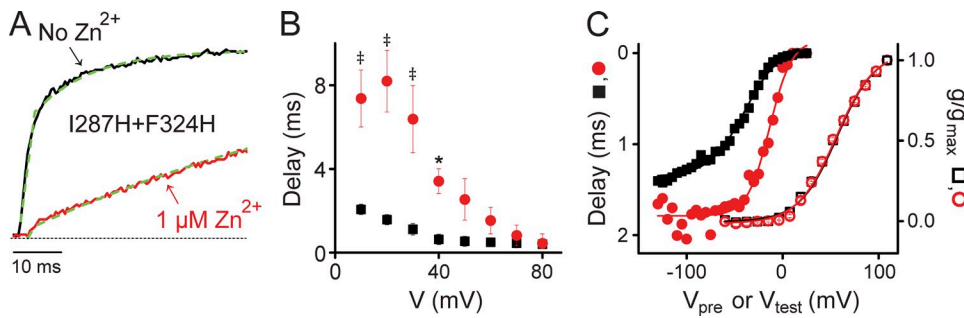
Figure 3. Extracellular Zn^{2+} delays pore opening in I287H+F324H channels. (A) Representative current traces, evoked by depolarizing from −80 to +40 mV in the absence (black) or presence (red) of 1 µM Zn^{2+}, are shown on an expanded scale to illustrate the effect of Zn^{2+} on the delay before pore opening. Delays were determined by extrapolating fitted single-exponential functions (dashed green lines) to the zero current level (dashed gray line) (Perozo et al., 1994; Lin et al., 2010). (B) The delay before pore opening was measured at test voltages ranging from +10 to +80 mV in the absence (black squares) or presence (red circles) of 1 µM Zn^{2+}. Delay values differed significantly in the presence and absence of Zn^{2+}, as indicated (*, P < 0.05; ‡, P < 0.005). Values are shown as mean ± SEM (n = 4–10). At +40 mV, delays measured with and without Zn^{2+} were 3.4 ± 0.6 ms and 0.6 ± 0.2 ms, respectively. (C) Zn^{2+} shifts the dependence of the delay on prepulse potential in the depolarized direction. Delay values have been plotted on an inverted scale as a function of prepulse potential. Delays were measured in the absence (black squares) or presence (red circles) of 1 µM Zn^{2+} by stepping from the holding potential of −80 mV to prepulse voltages ranging from −130 to 25 mV for 20 ms before depolarizing to +60 mV. Delay data were fitted with single Boltzmann functions (solid lines). Values of $V_{1/2}$ and slope were −39 ± 1 mV and 18 ± 1 mV, and −14 ± 3 mV and 12 ± 2 mV, respectively, in the absence and presence of Zn^{2+} (n = 6–8). Normalized conductance values, measured as a function of test potential in the absence (open black squares) or presence (open red circles) of Zn^{2+}, are shown on the same axes. Conductance data fitted with single Boltzmann functions (solid lines) with (red) or without (black) Zn^{2+} did not differ significantly. Values of $V_{1/2}$ and slope were 44 ± 1 mV and 17 ± 1 mV, and 43 ± 1 mV and 18 ± 1 mV, respectively, in the absence and presence of Zn^{2+} (n = 5). For clarity, error bars have been omitted from the figure.

mutations of key residues in the voltage sensor domain, and determined the effect of extracellular Zn^{2+} on channel activation. To verify that I287H can be accessed by Zn^{2+}, we mutated I287 and F324, which are analogous to the binding site residues in eag, to histidine and investigated the effects of extracellular Zn^{2+} on channel kinetics (Silverman et al., 2000; Lin et al., 2010). The addition of 1 µM Zn^{2+} dramatically slowed channel opening (Fig. 2, A and B). The half-maximal effective concentration of Zn^{2+} ($[Zn^{2+}]_{1/2}$) in I287H+F324H was 120 nM (Fig. 2 C). In contrast, Zn^{2+} had little or no effect on activation kinetics in the Shaker-IR parent channel or the I287H or F324H single mutants (Fig. 2 D).

In I287H+F324H, Zn^{2+} increased the delay before channel opening and shifted the dependence of the delay on prepulse voltage in the depolarized direction (Fig. 3, A–C). In contrast, Zn^{2+} had no significant effect on the conductance–voltage curve (Fig. 3 C). The delay before channel opening arises from nonrate-limiting conformational changes of the voltage sensor domain that occur early in the activation pathway, including transitions from the resting state to the penultimate closed state (Perozo et al., 1994; Lin et al., 2010). The effect of Zn^{2+} on the delay indicates that the ion can access the site at rest and that binding stabilizes the resting conformation (Lin et al., 2010).

Extracellular Zn^{2+} binds to I287H+R1H in a state-dependent manner

Previous studies suggest that R1 in S4 is in proximity to E1 and I287 in S2 in the resting conformation (Starace and Bezanilla, 2004; Tombola et al., 2005; Campos et al., 2007). To probe the state dependence of proximity between I287

and R1, we made the I287H+R1H double mutant and recorded ionic currents in the presence and absence of extracellular Zn^{2+} (Fig. 4). The addition of Zn^{2+} generated a slow kinetic component of activation that was prominent in the presence of a saturating concentration of Zn^{2+} (50 µM; Fig. 4 A). As a result, currents recorded in Zn^{2+} were not well fitted by a single-exponential component (Fig. 4 B). In contrast, Zn^{2+} had little effect on activation kinetics in the R1H single mutant (see Fig. 5 A).

Zn^{2+}-binding conformation in I287H+R1H is not the resting state

I287H+R1H current traces were fitted with the sum of two exponential functions to obtain estimates for the time constants, τ_{fast} and τ_{slow}, and their amplitudes, A_{fast} and A_{slow} (Fig. 5 A). Normalized A_{slow} values were plotted versus Zn^{2+} concentration (Fig. 5 B). The data were
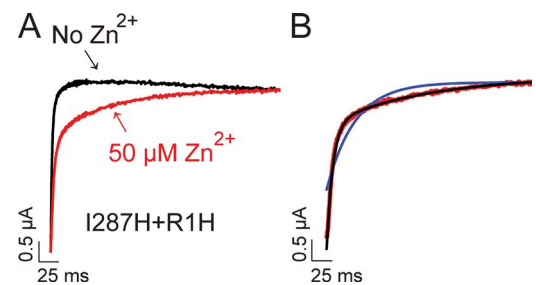

Figure 4. Zn^{2+} induces a slow component of activation in I287H+R1H channels. (A) Currents were evoked by depolarizing from −80 to +60 mV in the absence (black) or presence (red) of 50 µM Zn^{2+}. (B) Current trace obtained at +60 mV in the presence of Zn^{2+} (red) has been fitted with one (blue line) or the sum of two (black line) exponential functions.
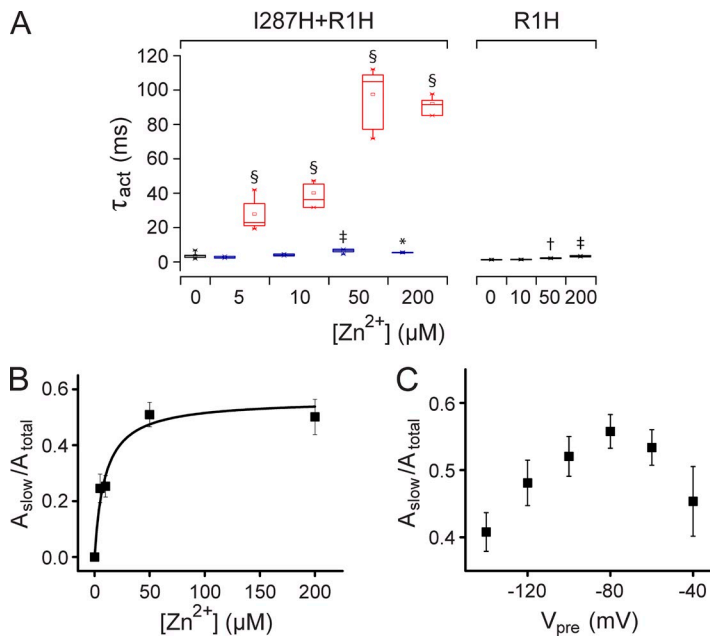
Figure 5. A subset of I287H+R1H voltage sensors binds Zn^{2+} at −80 mV. (A) The box plot shows τ_{act} values measured at +60 mV in the indicated concentrations of Zn^{2+} for I287H+R1H and the R1H single-mutant channel. I287H+R1H current traces were fitted with a single-exponential function in the absence of Zn^{2+} (black box, τ_{act}) and the sum of two exponential functions in the presence of Zn^{2+} (blue boxes, τ_{fast}; red boxes, τ_{slow}). R1H current traces were fitted with a single-exponential function in the presence and absence of Zn^{2+} (black boxes, τ_{act}). Mean values of τ_{act}, τ_{fast}, or τ_{slow} that differed significantly from no Zn^{2+} are indicated: *, $P < 0.05$; †, $P < 0.01$; ‡, $P < 0.005$; §, $P < 0.0005$ ($n = 3$–13). (B) The normalized amplitude of the slow component of activation measured at +60 mV in I287H+R1H channels has been plotted versus Zn^{2+} concentration ($n = 4$–7). The data were fitted with a rectangular hyperbola (black line) to obtain values for $[Zn^{2+}]_{1/2}$ and $A_{slow,max}$, which were 9.4 µM and 0.56, respectively. (C) $A_{slow,max}$ was measured as a function of prepulse voltage in the presence of a saturating Zn^{2+} concentration (200 µM; $n = 4$–7). The membrane was stepped from −80 mV to prepulse voltages ranging from −140 to −40 mV for 1 s before depolarizing to +80 mV.

fitted with a rectangular hyperbola to provide values for $[Zn^{2+}]_{1/2}$ (9.4 µM) and $A_{slow,max}$, the normalized maximum slow component amplitude. Interestingly, $A_{slow,max}$ approached ~56% at saturating Zn^{2+} concentrations (Fig. 5 B). This result strongly suggests that at −80 mV, the holding potential during the experiment, only a

fraction of the voltage sensors are in a conformation in which I287H and R1H are in proximity and able to form a binding site for extracellular Zn^{2+}.

In a population of channels, the distribution of voltage sensor conformations is controlled by membrane potential. To determine whether the Zn^{2+}-binding conformation
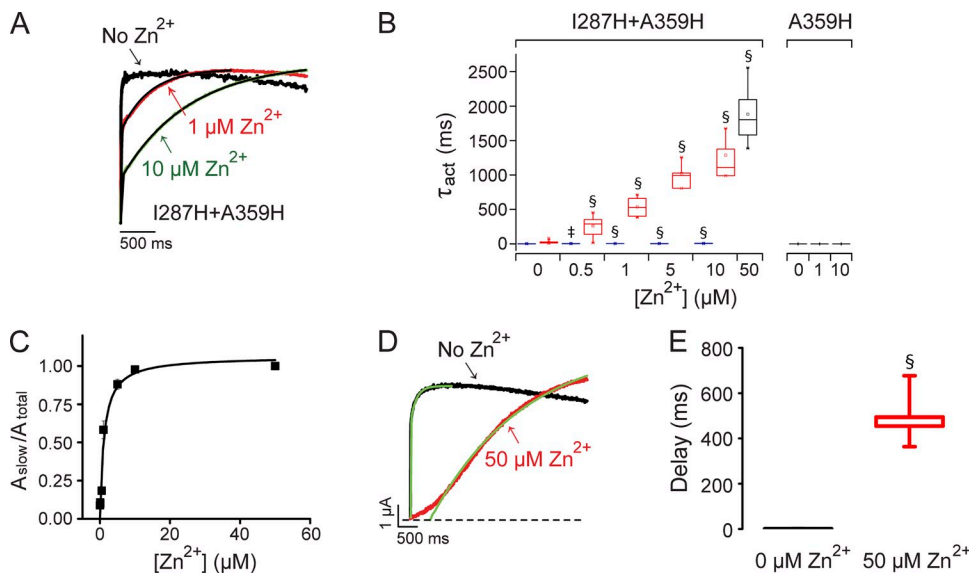

Figure 6. Extracellular Zn^{2+} slows activation and delays pore opening in I287H+A359H channels. (A) At subsaturating concentrations, Zn^{2+} induced a slow component of activation in I287H+A359H channels. The membrane was depolarized from −80 to +60 mV for 2 s. Representative current traces recorded in the presence or absence of Zn^{2+} (black, 0 µM; red, 1 µM; green, 10 µM) were scaled to the same amplitude, overlaid, and fitted with one (no Zn^{2+}) or the sum of two (+Zn^{2+}) exponential functions (black lines). (B) The box plot shows τ_{act} values measured at +60 mV in the indicated concentrations of Zn^{2+} for I287H+A359H and the A359H single-mutant channel. I287H+A359H current traces were fitted with the sum

of two exponential functions (blue boxes, τ_{fast}; red boxes, τ_{slow}), except at 50 µM Zn^{2+}, where one component was sufficient (black box, τ_{act}). A359H current traces were fitted with a single-exponential function (black boxes, τ_{act}). Mean values of τ_{act}, τ_{fast}, or τ_{slow} that differed significantly from no Zn^{2+} are indicated: ‡, $P < 0.005$; §, $P < 0.0005$ ($n = 3$–25). (C) The normalized amplitude of the slow component of activation measured at +60 mV has been plotted versus Zn^{2+} concentration ($n = 3$–10). The data were fitted with a rectangular hyperbola (black line) to obtain values for $[Zn^{2+}]_{1/2}$ and $A_{slow,max}$, which were 1.2 µM and 1.0, respectively. (D) Zn^{2+} increases the delay before pore opening. Representative current traces, evoked at +60 mV in the absence (black) or presence (red) of a saturating concentration (50 µM) of Zn^{2+}, were fitted with single-exponential functions (green). The fitted functions were extrapolated to the zero current level (dashed line) to estimate the delay (Perozo et al., 1994; Lin et al., 2010). (E) The box plot shows the delay before pore opening measured in the absence (black box) or presence (red box) of 50 µM Zn^{2+}. Mean values obtained at +60 mV were 496 ± 50 ms and 0.8 ± 0.1 ms, with and without Zn^{2+}, respectively, and differed significantly (§, $P < 0.0005$; $n = 5$–9).

in I287H+R1H corresponds to the resting state, we investigated the effect of prepulse voltage on $A_{slow,max}$ measured in the presence of a saturating concentration of Zn^{2+}. The membrane was stepped from the holding potential of -80 mV to prepulse voltages ranging from -140 to -40 mV for 1 s before depolarizing to +80 mV. Current traces were fitted with the sum of two exponential functions to estimate $A_{slow,max}$. We found that $A_{slow,max}$ decreased after both depolarizing and hyperpolarizing prepulses (Fig. 5 C). These data indicate that changing the membrane potential in either direction separates R1H and I287H, precluding Zn^{2+} binding. The decrease in $A_{slow,max}$ after depolarizing prepulses is readily explained. Depolarization would be expected to move R1 toward the extracellular side of the membrane, away from I287. The more surprising result is that prepulse hyperpolarization also reduced $A_{slow,max}$. These data are incompatible with the idea that Zn^{2+} binds to the resting state in I287H+R1H. In that case, the value of $A_{slow,max}$ would be expected to increase upon hyperpolarization because more voltage sensors would be drawn down into the resting, ion-binding conformation. In contrast, the decrease in $A_{slow,max}$ upon hyperpolarization provides strong evidence that R1 moves further inward toward the gating charge transfer center in the resting state. With R1H located below F290, the ion-binding site would be disrupted.

I287H forms a binding site with A359H, located in the S3–S4 loop

If I287H+R1H voltage sensors are unable to bind Zn^{2+} in the resting state because R1H is located in the gating charge transfer center, residues in the S3–S4 loop may be pulled into the plane of the membrane in the resting

conformation. To investigate this possibility, we made the I287H+A359H double mutant and recorded ionic currents in the presence and absence of extracellular Zn^{2+}. Position A359 is three residues N-terminal to R1 (R362) in Shaker (Fig. 1 A) (Tempel et al., 1987). The addition of a subsaturating concentration of Zn^{2+} generated a slow kinetic component of activation (Fig. 6 A). Currents recorded in 10 µM Zn^{2+} or less were not well fitted by a single-exponential component. In contrast, the A359H single mutant was not significantly affected by extracellular Zn^{2+} (Fig. 6 B).

I287H+A359H current traces were fitted with the sum of two exponential functions (Fig. 6 B). Normalized A_{slow} values were plotted versus Zn^{2+} concentration (Fig. 6 C). The data were fitted with a rectangular hyperbola to provide values for $[Zn^{2+}]_{1/2}$ (1.2 µM) and $A_{slow,max}$. In a saturating concentration of Zn^{2+} (50 µM), $A_{slow,max}$ reached 100% (Fig. 6 C). These results indicate that Zn^{2+} binding in I287H+A359H traps the voltage sensor in an absorbing conformation. To bind Zn^{2+}, A359H must be in proximity to I287H. This strongly suggests that, in the ion-binding conformation, R1 has moved further toward the intracellular side of the membrane. These results are consistent with the conclusion that R1 is located in the gating charge transfer center in the resting conformation.

If Zn^{2+} traps the I287H+A359H voltage sensor in the resting conformation, ion binding would be expected to increase the delay before channel opening. We measured the delay in a saturating concentration of Zn^{2+} (50 µM) so that activation kinetics could be fitted reasonably well with a single-exponential function (Fig. 6 D). The addition of Zn^{2+} dramatically increased the delay before pore opening (Fig. 6 E). Because activation was
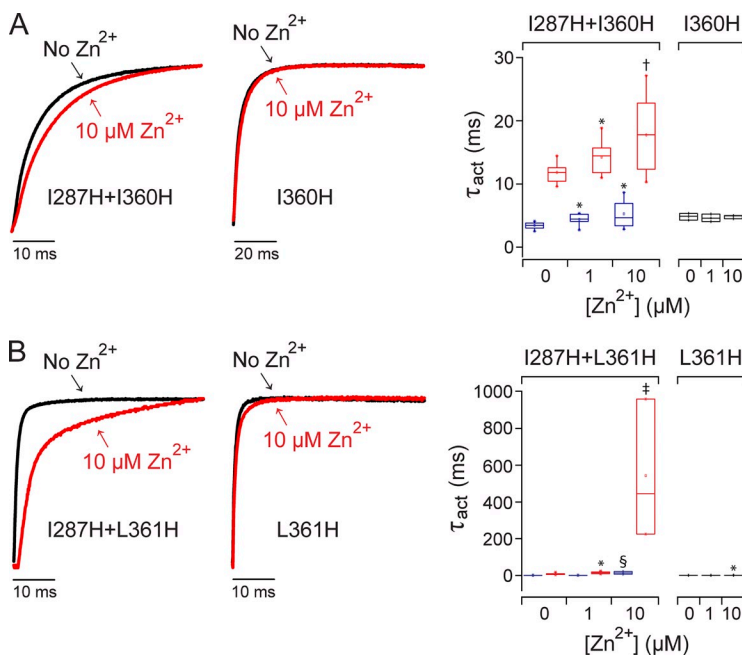

Figure 7. Effects of Zn^{2+} on channels containing I287H paired with histidine mutations in the S3–S4 loop. (A; left) I127H+I360H double mutant. (Middle) I360H single mutant. (B; left) I127H+L361H double mutant. (Middle) L361H single mutant. Currents were evoked by pulsing from -80 to +60 mV in the absence (black) or presence of 10 µM Zn^{2+} (red). Representative current traces have been scaled to the same amplitude and overlaid. At right, the box plots show τ_{act} values measured at +60 mV in the indicated concentrations of Zn^{2+} for (A) I287H+I360H and the I360H single-mutant channel or (B) I287H+L361H and the L361H single-mutant channel. Double-mutant current traces were fitted with the sum of two exponential functions (blue boxes, τ_{fast}; red boxes, τ_{slow}). Single-mutant current traces were fitted with a single-exponential function (black boxes, τ_{act}). Mean values of τ_{act}, τ_{fast}, or τ_{slow} that differed significantly from no Zn^{2+} are indicated: *, P < 0.05; †, P < 0.01; ‡, P < 0.005; §, P < 0.0005 (n = 3–10).

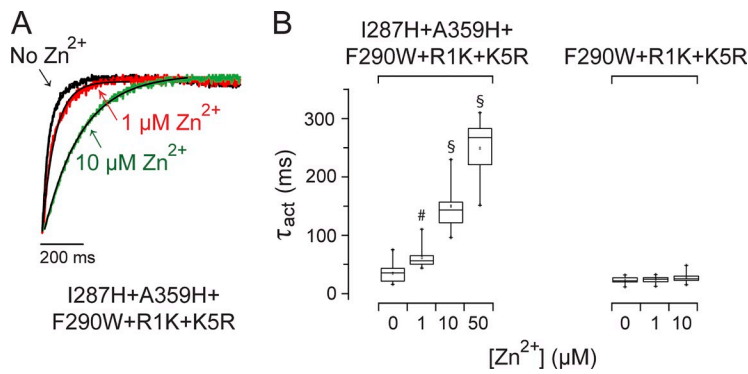**Figure 8.** Zn^{2+} slows activation in I287H+A359H+F290W+R1K+K5R channels. (A) Currents were evoked by depolarizing to +60 mV in the absence or presence of Zn^{2+}: black, 0 µM; red, 1 µM; green, 10 µM. Traces have been scaled to the same amplitude and overlaid. Currents were fitted with one exponential component (black lines) to obtain values for τ_{act}. (B) The box plot shows values of τ_{act} measured at +60 mV in I287H+A359H+F290W+R1K+K5R or the F290W+R1K+K5R control channel as a function of Zn^{2+} concentration. Mean values of τ_{act} that differed significantly from no Zn^{2+} are indicated: #, $P < 0.001$; §, $P < 0.0005$ ($n = 6$–15).

extremely slow in 50 µM Zn^{2+} (see Fig. 6 B), it was not feasible to study the dependence of the delay on prepulse voltage.

We also investigated the effect of Zn^{2+} on activation kinetics in I287H+I360H and I287H+L361H (Fig. 7). I360 and L361 are located between A359 and R1 (Tempel et al., 1987). With or without Zn^{2+}, the activation kinetics of I287H+I360H and I287H+L361H were best fitted by the sum of two exponential components, providing estimates for τ_{fast} and τ_{slow}. We found that 10 µM Zn^{2+} increased τ_{slow} substantially in I287H+L361H, whereas 10 µM Zn^{2+} had a less dramatic effect on τ_{slow} in I287H+I360H (Fig. 7, A and B). Because L361 is immediately adjacent to R1 in the linear sequence, the ion-binding conformation in I287H+L361H may be similar to that in I287H+R1H. The finding that I287H is able to form Zn^{2+}-binding sites with A359H, L361H, and R1H suggests that the directions of these side chains are not rigidly fixed. This may reflect the conformational flexibility of the S4 segment, which can adopt either 3_{10}- or α-helical secondary structures (Long et al., 2007).

Stabilizing the resting state enhances Zn^{2+} binding in I287H+A359H

If I287H+A359H binds Zn^{2+} at rest, stabilizing the resting state should enhance binding. To test this prediction, we transferred the I287H+A359H binding site into the F290W+R1K+K5R triple-mutant background, which stabilizes the resting voltage sensor conformation (Tao et al., 2010). In the triple-mutant background,

Zn^{2+} binding to the I287H+A359H site significantly slowed channel activation (Fig. 8 A). In contrast to I287H+A359H in the wild-type background, activation kinetics were well fitted by a single-exponential component, even in subsaturating concentrations of Zn^{2+} (Fig. 8, A and B). Therefore, at −80 mV, a large fraction of the voltage sensors were in the ion-binding conformation, that is, with A359H and I287H in proximity to each other. This is compatible with the finding that the bulk of the gating charge in F290W+R1K+K5R moves at voltages positive to −70 mV (Tao et al., 2010). This indicates that most voltage sensor domains are in the resting state at −80 mV, which corresponds to the ion-binding conformation in I287H+A359H.

DISCUSSION

Our results strongly support the conclusion that R1 in the Shaker S4 segment occupies the gating charge transfer center in the resting voltage sensor conformation (Fig. 9 A). To investigate the position of R1, we took advantage of the I287H mutation, which can be used to generate Zn^{2+}-binding sites in or near the pathway of S4 movement (Silverman et al., 2000; Lin et al., 2010). Ion binding directly modulates voltage sensor conformational changes (Tang et al., 2000; Silverman et al., 2004; Bannister et al., 2005; Lin et al., 2010). Importantly, binding sites involving I287H are accessible in the resting state and are located extracellular to the charge transfer center. It is worth noting that the relative positions
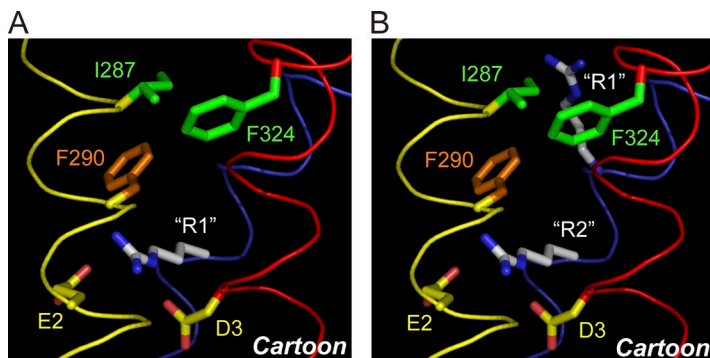

Figure 9. R1 in S4 occupies the gating charge transfer center in the resting state. (A) Cartoon of the resting conformation shows an arginine representing R1 in the gating charge transfer center. (A and B) Ribbons representing the backbone atoms of S2, S3, and S4 are shown in yellow, red, and blue, respectively. Backbone atoms and side chains corresponding to I287, F290, E2, D3, and F324 (mutated in silico from tryptophan) in Shaker were extracted from the Kv1.2/Kv2.1 paddle chimera x-ray structure (2r9r) (Long et al., 2007). (B) Cartoon of the penultimate closed state shows arginines representing R1 in the vicinity of I287 and R2 in the gating charge transfer center. Other side chains and colored ribbons are the same as in A. The figure was made with PyMOL (v1.3).

of I287 and the charge transfer center are not likely to change during voltage-dependent activation because I287 and F290 are separated by only two residues in the linear sequence (Tempel et al., 1987).

We identified an ion-binding conformation in I287H+R1H that was maximally occupied at -80 mV. The fraction of voltage sensors capable of binding Zn^{2+} was reduced at either more positive or more negative voltages. These data suggest that R1H moves far enough outward or inward to abolish ion binding, going beyond the point where reorientation of the I287H and R1H side chains would be able to reestablish a binding site. It is likely that this requires movement of the S4 backbone. Our results are incompatible with the notion that R1 is close to I287 in the resting state, but are consistent with the idea that R1 and I287 are in proximity in an intermediate closed state in the activation pathway (Fig. 9 B).

In contrast, we found that Zn^{2+} bound to an absorbing conformation in I287H+A359H. A359 is located in the S3–S4 loop, extracellular to R1. Formation of a binding site between I287H and A359H indicates that the S4 segment has moved inward compared with I287H+R1H, drawing R1 down into the gating charge transfer center. Importantly, our results support the conclusion that R1 occupies the gating charge transfer center during activation of the wild-type channel because entry of R1 into this position does not require the F290W+R1K+K5R triple-mutant combination (Tao et al., 2010). However, transferring I287H+A359H into the triple-mutant background enhanced Zn^{2+} binding, consistent with the conclusion that the ion-binding conformation corresponds to the resting state.

Extracellular Zn^{2+} bound to the resting conformation in I287H+F324H and I287H+A359H with $[Zn^{2+}]_{1/2}$ values of 0.12 and 1.2 µM, respectively. These high apparent affinities suggest that the binding site residues are in atomic proximity of one another at rest (Lainé et al., 2003). In I287H+R1H, $[Zn^{2+}]_{1/2}$ was larger, 9.4 µM. This lower apparent affinity is compatible with our evidence that I287H+R1H voltage sensors can adopt two or more conformations at -80 mV, only one of which can bind Zn^{2+}. However, we cannot rule out the possibility that the binding site residues are closer to each other in I287H+F324H and I287H+A359H than they are in I287H+R1H.

To initiate outward S4 movement from the resting state, R1 in the charge transfer center must be within the transmembrane electric field. A recent refinement of the Kv1.2 x-ray structure identified a highly conserved hydrophobic layer, $\sim$10-Å thick, in the voltage sensor domain where the transmembrane electric field is likely to be focused (Chen et al., 2010). This layer comprises 10 residues in S1, S2 (including F290), and S3a, regions that are thought to remain stationary relative to S4 during activation gating. The location of the hydrophobic layer

is consistent with the idea that R1 experiences part of the transmembrane field in the resting conformation. Our results are compatible with a mechanism for voltage gating in Shaker in which R1 and K5 occupy the charge transfer center in the resting and activated states, respectively, and R2, R3, and R4 pass through this region during intermediate conformational changes.

The predominant conformation of S4 at negative voltages may be readily affected by R1 mutations, particularly neutralizations. If R1 is replaced by a neutral amino acid, S4 may be less likely to retract as far as it does in the wild-type channel. This could explain why some previous results suggest that R1 is near E1 and I287 in S2 and I241 in S1 in the resting state (Starace and Bezanilla, 2004; Tombola et al., 2005; Campos et al., 2007). In such mutants, R2 may be the primary occupant of the charge transfer center at hyperpolarized potentials (see Fig. 9 B). This would place R2 in the electric field, where it could initiate outward S4 movement upon depolarization (Chen et al., 2010).

Interestingly, S4 segments in a variety of voltage-gated ion channels contain different numbers of positively charged amino acids. For instance, Kv2.1 has a glutamine in the R1 position (Long et al., 2007). Depending on its sequence, the register of S4 in its maximally retracted position may differ. This raises the possibility that the structure of the resting conformation in voltage-gated channels varies depending on which S4 residue occupies the charge transfer center.

REFERENCES

Aggarwal, S.K., and R. MacKinnon. 1996. Contribution of the S4 segment to gating charge in the Shaker K$^+$ channel. *Neuron.* 16:1169–1177. doi:10.1016/S0896-6273(00)80143-9

Bannister, J.P.A., B. Chanda, F. Bezanilla, and D.M. Papazian. 2005. Optical detection of rate-determining ion-modulated conformational changes of the ether-à-go-go K$^+$ channel voltage sensor. *Proc. Natl. Acad. Sci. USA.* 102:18718–18723. doi:10.1073/pnas.0505766102

Campos, F.V., B. Chanda, B. Roux, and F. Bezanilla. 2007. Two atomic constraints unambiguously position the S4 segment relative to S1 and S2 segments in the closed state of Shaker K channel. *Proc. Natl. Acad. Sci. USA.* 104:7904–7909. doi:10.1073/pnas.0702638104

Chen, X., Q. Wang, F. Ni, and J. Ma. 2010. Structure of the full-length Shaker potassium channel Kv1.2 by normal-mode-based X-ray crystallographic refinement. *Proc. Natl. Acad. Sci. USA.* 107:11352–11357. doi:10.1073/pnas.1000142107

Hoshi, T., W.N. Zagotta, and R.W. Aldrich. 1990. Biophysical and molecular mechanisms of Shaker potassium channel inactivation. *Science.* 250:533–538. doi:10.1126/science.2122519

Islas, L.D., and F.J. Sigworth. 1999. Voltage sensitivity and gating charge in *Shaker* and *Shab* family potassium channels. *J. Gen. Physiol.* 114:723–742. doi:10.1085/jgp.114.5.723

Khalili-Araghi, F., V. Jogini, V. Yarov-Yarovoy, E. Tajkhorshid, B. Roux, and K. Schulten. 2010. Calculation of the gating charge for the Kv1.2 voltage-activated potassium channel. *Biophys. J.* 98:2189–2198. doi:10.1016/j.bpj.2010.02.056

Lainé, M., M.C. Lin, J.P.A. Bannister, W.R. Silverman, A.F. Mock, B. Roux, and D.M. Papazian. 2003. Atomic proximity between S4 segment and pore domain in Shaker potassium channels. *Neuron.* 39:467–481. doi:10.1016/S0896-6273(03)00468-9

Lin, M.C., J. Abramson, and D.M. Papazian. 2010. Transfer of ion binding site from ether-à-go-go to Shaker: Mg^{2+} binds to resting state to modulate channel opening. *J. Gen. Physiol.* 135:415–431. doi:10.1085/jgp.200910320

Long, S.B., X. Tao, E.B. Campbell, and R. MacKinnon. 2007. Atomic structure of a voltage-dependent K^+ channel in a lipid membrane-like environment. *Nature.* 450:376–382. doi:10.1038/nature06265

Papazian, D.M., L.C. Timpe, Y.N. Jan, and L.Y. Jan. 1991. Alteration of voltage-dependence of Shaker potassium channel by mutations in the S4 sequence. *Nature.* 349:305–310. doi:10.1038/349305a0

Pathak, M.M., V. Yarov-Yarovoy, G. Agarwal, B. Roux, P. Barth, S. Kohout, F. Tombola, and E.Y. Isacoff. 2007. Closing in on the resting state of the Shaker K^+ channel. *Neuron.* 56:124–140. doi:10.1016/j.neuron.2007.09.023

Perozo, E., L. Santacruz-Toloza, E. Stefani, F. Bezanilla, and D.M. Papazian. 1994. S4 mutations alter gating currents of Shaker K channels. *Biophys. J.* 66:345–354. doi:10.1016/S0006-3495(94)80783-0

Schoppa, N.E., K. McCormack, M.A. Tanouye, and F.J. Sigworth. 1992. The size of gating charge in wild-type and mutant Shaker potassium channels. *Science.* 255:1712–1715. doi:10.1126/science.1553560

Seoh, S.A., D. Sigg, D.M. Papazian, and F. Bezanilla. 1996. Voltage-sensing residues in the S2 and S4 segments of the Shaker K^+ channel. *Neuron.* 16:1159–1167. doi:10.1016/S0896-6273(00)80142-7

Silverman, W.R., C.-Y. Tang, A.F. Mock, K.-B. Huh, and D.M. Papazian. 2000. Mg^{2+} modulates voltage-dependent activation in ether-à-go-go potassium channels by binding between transmembrane segments S2 and S3. *J. Gen. Physiol.* 116:663–678. doi:10.1085/jgp.116.5.663

Silverman, W.R., J.P.A. Bannister, and D.M. Papazian. 2004. Binding site in eag voltage sensor accommodates a variety of ions and is accessible in closed channel. *Biophys. J.* 87:3110–3121. doi:10.1529/biophysj.104.044602

Starace, D.M., and F. Bezanilla. 2004. A proton pore in a potassium channel voltage sensor reveals a focused electric field. *Nature.* 427:548–553. doi:10.1038/nature02270

Tang, C.-Y., F. Bezanilla, and D.M. Papazian. 2000. Extracellular Mg^{2+} modulates slow gating transitions and the opening of *Drosophila* ether-à-go-go potassium channels. *J. Gen. Physiol.* 115:319–338. doi:10.1085/jgp.115.3.319

Tao, X., A. Lee, W. Limapichat, D.A. Dougherty, and R. MacKinnon. 2010. A gating charge transfer center in voltage sensors. *Science.* 328:67–73. doi:10.1126/science.1185954

Tempel, B.L., D.M. Papazian, T.L. Schwarz, Y.N. Jan, and L.Y. Jan. 1987. Sequence of a probable potassium channel component encoded at *Shaker* locus of *Drosophila. Science.* 237:770–775. doi:10.1126/science.2441471

Timpe, L.C., T.L. Schwarz, B.L. Tempel, D.M. Papazian, Y.N. Jan, and L.Y. Jan. 1988. Expression of functional potassium channels from *Shaker* cDNA in *Xenopus* oocytes. *Nature.* 331:143–145. doi:10.1038/331143a0

Tombola, F., M.M. Pathak, and E.Y. Isacoff. 2005. Voltage-sensing arginines in a potassium channel permeate and occlude cation-selective pores. *Neuron.* 45:379–388. doi:10.1016/j.neuron.2004.12.047

Yarov-Yarovoy, V., D. Baker, and W.A. Catterall. 2006. Voltage sensor conformations in the open and closed states in ROSETTA structural models of K^+ channels. *Proc. Natl. Acad. Sci. USA.* 103:7292–7297. doi:10.1073/pnas.0602350103